



Brazilian Journal of Physics

ISSN: 0103-9733

luizno.bjp@gmail.com

Sociedade Brasileira de Física

Brasil

Antunes, S. M.; Krein, G.; Vizcarra, V. E.  
Charmed-Meson Scattering on Nucleons in a QCD Coulomb Gauge Quark Model  
Brazilian Journal of Physics, vol. 37, núm. 1B, march, 2007, pp. 265-269  
Sociedade Brasileira de Física  
São Paulo, Brasil

Available in: <http://www.redalyc.org/articulo.oa?id=46437217>

- How to cite
- Complete issue
- More information about this article
- Journal's homepage in redalyc.org

redalyc.org

Scientific Information System  
Network of Scientific Journals from Latin America, the Caribbean, Spain and Portugal  
Non-profit academic project, developed under the open access initiative

## Charmed-Meson Scattering on Nucleons in a QCD Coulomb Gauge Quark Model

S. M. Antunes, G. Krein, and V.E. Vizcarra

Instituto de Física Teórica, Universidade Estadual Paulista, Rua Pamplona 145, 01405-900 São Paulo, SP, Brazil

(Received on 28 November, 2006)

The scattering of charmed mesons on nucleons is investigated within a chiral quark model inspired on the QCD Hamiltonian in Coulomb gauge. The microscopic model incorporates a longitudinal Coulomb confining interaction derived from a self-consistent quasi-particle approximation to the QCD vacuum, and a transverse hyperfine interaction motivated from lattice simulations of QCD in Coulomb gauge. From the microscopic interactions at the quark level, effective meson-baryon interactions are derived using a mapping formalism that leads to quark-Born diagrams. As an application, the total cross-section of heavy-light  $D$ -mesons scattering on nucleons is estimated.

Keywords: Quantum chromodynamics; Coulomb gauge; Quark model; Charmed mesons; Hadron-hadron interactions

### I. INTRODUCTION

The study of the interactions of charmed hadrons with normal hadrons is of interest in several instances. One example refers to experiments of relativistic heavy ion collisions (RHIC). Since the early suggestion of Matsui and Satz [1] that the suppression of  $J/\Psi$  production in RHIC could provide a signature of quark-gluon deconfinement, the importance of charmonium interaction with normal nuclear matter hadrons has attracted much attention [2]. Another example is the understanding and identification of the effective degrees of freedom that are responsible for dynamical chiral symmetry breaking and the confinement of quarks and gluons in hadrons. Heavy-light mesons, like the  $D$ -mesons, are sometimes considered as the hydrogen atom of QCD. This is so because the charm quark  $c$  is much heavier than the light  $u$  and  $d$  quarks, and to a good approximation these mesons can be described as one-body bound states. Moreover, since the properties of  $u$  and  $d$  quarks are determined by the dynamical breaking of chiral symmetry, the interaction of these quarks with a heavy color source, as the  $c$  quark, can provide valuable information on the properties of the QCD interaction at the confinement regime. Also, recent results for  $J/\Psi$  dissociation cross sections obtained using SU(4) symmetric meson-exchange models [3] indicate that these models provide cross sections that are one order of magnitude smaller than those calculated using quark models [2]. This is an important issue, the reasons for such discrepancies should be understood.

In the present communication we report on an ongoing study of the interaction of charmed  $D$ -mesons on nucleons using a microscopic quark model inspired on the Hamiltonian of QCD in the Coulomb gauge. Specifically, the microscopic model incorporates a longitudinal Coulomb confining interaction derived from a self-consistent quasi-particle approximation to the QCD vacuum [4], and a transverse hyperfine interaction motivated from lattice simulations of QCD in Coulomb gauge [5]. Given the microscopic quark Hamiltonian, we solve a gap equation for the constituent quark mass function and obtain the bound states of  $D$  mesons and of nucleons. This is done by using a low-energy approximation of the full Bethe-Salpeter bound-state kernels and using an ansatz for the Fock-space meson amplitudes. Once the bound-state amplitudes of the mesons and the nucleons are obtained, we employ

the Fock-Tani mapping formalism [6] of Refs. [7–9] to obtain an effective meson-nucleon Hamiltonian describing quark interchange between the mesons and baryons. This approach gives equivalent results as the quark-Born diagram formalism of Barnes and Swanson [10]. As an illustration of the formalism, we calculate the total cross section for the process  $p + \bar{D}^0 \rightarrow p + \bar{D}^0$ . We also calculate the same cross section using as microscopic interaction the hyperfine component of one-gluon-exchange, which is traditionally used in the context of nonrelativistic quark models.

The paper is organized as follows. In the next Section we discuss the microscopic quark model based on the Hamiltonian in Coulomb gauge QCD, and obtain the gap equation that gives the constituent quark mass function. In Section III we use obtain the effective meson-baryon interaction using a low energy approximation of the interaction. Numerical results are presented in Section IV and our Conclusions and Perspectives are presented in Section V.

### II. THE MICROSCOPIC QUARK MODEL

The model Hamiltonian we use is given by [11]

$$H = H_q + H_C + H_T, \quad (1)$$

with

$$H_q = \int d^3x \psi^\dagger(x) [-i\alpha \cdot \nabla + \beta m_0] \psi(x), \quad (2)$$

$$H_C = -\frac{1}{2} \int d^3x d^3y \rho^a(x) V(|x-y|) \rho^a(x), \quad (3)$$

$$H_T = \frac{1}{2} \int d^3x d^3y J_i^a(x) U_{ij}(|x-y|) J_j^a(x) \quad (4)$$

In these expressions,  $\psi(x)$  is the quark field operator (with color and flavor indices suppressed) and  $m_0 = m_u, m_d, \dots$  is the current quark mass matrix. In addition, the quark charge and current densities  $\rho^a(x)$  and  $J^a(x)$  are given by

$$\rho^a(x) = \psi^\dagger(x) T^a \psi(x), \quad J^a(x) = \psi^\dagger(x) T^a \alpha \psi(x), \quad (5)$$

where  $T^a = \lambda^a/2$ ,  $a = 1, \dots, 8$ , with  $\lambda^a$  the SU(3) Gell-Mann matrices. The Coulomb and transverse potentials  $V$  and  $U$  will be discussed in Section IV.

One can approximately diagonalize the effective quark Hamiltonian using a BCS treatment for quark field operators. One way to implement this is as follows. Initially one expands the quark field operators as

$$\Psi(x) = \int \frac{d^3k}{(2\pi)^{3/2}} \sum_{s=\pm 1/2} [u_s(k)q_s(k) + v_s(k)\bar{q}_s(-k)] e^{ik \cdot x}, \quad (6)$$

where  $q_s(k)$  and  $\bar{q}_s(k)$  are creation and annihilation operators, and

$$u_s(k) = \sqrt{\frac{E_k + M_k}{2E_k}} \begin{pmatrix} 1 \\ \frac{\sigma \cdot k}{E_k + M_k} \end{pmatrix} \chi_s, \quad (7)$$

$$v_s(k) = \sqrt{\frac{E_k + M_k}{2E_k}} \begin{pmatrix} -\frac{\sigma \cdot k}{E_k + M_k} \\ 1 \end{pmatrix} \chi_s^c, \quad (8)$$

where  $E_k = (k^2 + M_k^2)^{1/2}$ ,  $\chi_s^c = -i\sigma^2 \chi_s$ , and  $\chi_s$  is a Pauli spinor. Next, one substitutes this into the Hamiltonian and uses Wick contraction techniques so that it can be rewritten as

$$H = H_0 + H_2 + H_4, \quad (9)$$

where  $H_0$  is a c-number and  $H_2$  ( $H_4$ ) contains normal ordered terms with products of two (four) creation and/or annihilation operators. The last step consists in demanding that  $H_2$  is in diagonal form. This implies that  $M_k$  must satisfy the following gap equation

$$M_k = m_0 + \frac{2}{3} \int \frac{d^3q}{(2\pi)^3} \left[ \frac{f_1(k, q)V(|k-q|) - g_1(k, q)U(|k-q|)}{E_q} \right], \quad (10)$$

with

$$f_1(k, q) = M_k \frac{q}{k} \hat{k} \cdot \hat{q} - M_q, \quad (11)$$

$$g_1(k, q) = 2M_q + 2M_k \frac{q}{k} \frac{(k \cdot q - k^2)(k \cdot q - q^2)}{kq|k-q|^2}. \quad (12)$$

In addition, one finds that  $H_2$  is given as

$$H_2 = \int \frac{d^3k}{(2\pi)^3} \epsilon_k \sum_s \left[ q_s^\dagger(k)q_s(k) + \bar{q}_s^\dagger(k)\bar{q}_s(k) \right], \quad (13)$$

where

$$\epsilon_k = \frac{k^2 + m_0 M_k}{E_k} - \frac{2}{3} \int \frac{d^3q}{(2\pi)^3} \left[ \frac{f_2(k, q)V(|k-q|) + g_2(k, q)U(|k-q|)}{E_k E_q} \right], \quad (14)$$

with

$$f_2(k, q) = M_k M_q + k \cdot q, \quad (15)$$

$$g_2(k, q) = 2M_k M_q - 2 \frac{q}{k} \frac{(k \cdot q - k^2)(k \cdot q - q^2)}{|k-q|^2}. \quad (16)$$

Numerical solutions of the gap equation will be presented in Section IV. In the next Section, we discuss the derivation of an effective meson-baryon interaction.

### III. THE EFFECTIVE MESON-BARYON INTERACTION

The effective meson-baryon interaction will depend on the microscopic quark Hamiltonian  $H_4$  and the bound-state amplitudes of the mesons and baryons [7–10]. For heavy-light mesons and baryons, one can write the corresponding Fock-space states as follows [12]. For a one-meson state one can write,

$$|\alpha\rangle = M_\alpha^\dagger |\Omega\rangle = \Phi_\alpha^{\mu\nu} q_\mu^\dagger \bar{q}_\nu^\dagger |0\rangle, \quad (17)$$

where  $\Phi$  is the Fock-space amplitude, with  $\alpha$  indicating all quantum numbers necessary to specify the meson state, like c.m. momentum, spin and flavor, and  $\mu, \nu$  indicate the corresponding quantum numbers of the quarks and antiquarks – a sum or integral over repeated indices is implied. The state  $|0\rangle$  is the constituent-quark, chirally-broken vacuum state, i.e. the state annihilated by the constituent quark and antiquark annihilation operators  $q$  and  $\bar{q}$ . For a one-baryon state, one can write

$$|\alpha\rangle = B_\alpha^\dagger |\Omega\rangle = \frac{1}{\sqrt{3!}} \Psi_\alpha^{\mu_1 \mu_2 \mu_3} q_{\mu_1}^\dagger q_{\mu_2}^\dagger q_{\mu_3}^\dagger |0\rangle, \quad (18)$$

where  $\Psi$  is the Fock-space amplitude, and  $\alpha, \mu, \nu, \sigma$  have the same meaning as for the meson state. To simplify notation, we write the relevant piece of  $H_4$  in the form

$$H_4 = \frac{1}{2} V_{qq}(\mu\nu; \rho\sigma) q_\mu^\dagger q_\nu^\dagger q_\sigma q_\rho + \frac{1}{2} V_{\bar{q}\bar{q}}(\mu\nu; \rho\sigma) \bar{q}_\mu^\dagger \bar{q}_\nu^\dagger \bar{q}_\sigma \bar{q}_\rho + V_{q\bar{q}}(\mu\nu; \rho\sigma) q_\mu^\dagger \bar{q}_\nu^\dagger \bar{q}_\sigma q_\rho^\dagger, \quad (19)$$

where  $V_{qq}, \dots$  contain products of the Dirac spinors and the interactions  $V$  and  $U$ .

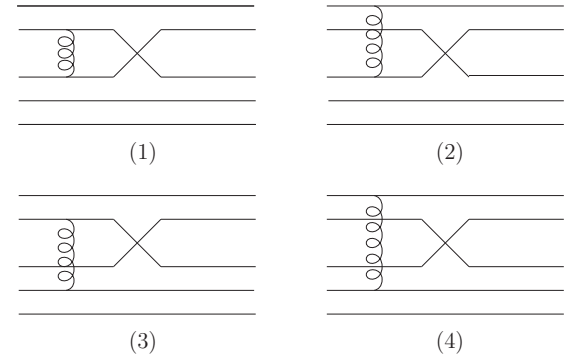


FIG. 1: Pictorial representation of the four different quark-interchange processes that contribute to the  $DN$  interaction.

In this paper we consider only quark interchange processes, i.e. those that do not involve valence  $q\bar{q}$  annihilation processes like  $p + \bar{D}^0 \rightarrow p + \bar{D}^0$ ,  $n + \bar{D}^0 \rightarrow p + D^-$ , etc. In Fig. 1 we present a pictorial representation of such quark interchange processes. In these graphs, the exchanged quarks are always the light  $u$  and  $d$  quarks, the  $c$  antiquarks are not interchanged with the light quarks of the baryons. The Fock-Tani mapping

procedure leads to the following expression for the effective  $DN$  interaction

$$V_{DN} = -3\Phi_{\alpha}^{*\mu\nu 1}\Psi^{*\nu\mu_2\mu_3}V_{qq}(\mu\nu;\sigma\rho)\Phi_{\gamma}^{\rho\nu 1}\Psi_{\delta}^{\sigma\mu_2\mu_3} \quad (20)$$

$$- 3\Phi_{\alpha}^{*\sigma\rho}\Psi^{*\mu_1\mu_2\mu_3}V_{q\bar{q}}(\mu\nu;\sigma\rho)\Phi_{\gamma}^{\mu_1\nu}\Psi_{\delta}^{\mu_2\mu_3} \quad (21)$$

$$- 6\Phi_{\alpha}^{*\mu_1\nu 1}\Psi^{*\nu\mu_2\mu_3}V_{qq}(\mu\nu;\sigma\rho)\Phi_{\gamma}^{\rho\nu 1}\Psi_{\delta}^{\mu_1\sigma\mu_3} \quad (22)$$

$$- 6\Phi_{\alpha}^{*\mu_1\nu}\Psi^{*\nu\mu_2\mu_3}V_{q\bar{q}}(\mu\nu;\sigma\rho)\Phi_{\gamma}^{\nu 1\rho}\Psi_{\delta}^{\mu_1\sigma\mu_3}. \quad (23)$$

In order to get insight into the problem and avoid massive numerical evaluation of multidimensional integrals, we use a low-energy expansion for  $H_4$  in Eq. (9) and use Gaussian ansätze for the Fock-space amplitudes  $\Phi$  and  $\Psi$ . Expanding  $M_k$  for small  $k$  as

$$M_k = M - M_1 k - M_2 k^2, \quad (24)$$

one can easily show that the quark spinors  $u$  and  $v$  can be written for small  $k$  as

$$u_s(k) \approx \left(1 - \frac{pk^2}{8M^2}\right) \chi_s, \quad (25)$$

$$v_s(k) = \left(1 - \frac{k^2}{8M^2}\right) \chi_s^c. \quad (26)$$

Replacing these into Eq. (19), one obtains a Hamiltonian that is like the Breit Hamiltonian of QED. The different pieces of the Hamiltonian contain momentum-dependent and -independent central interactions, spin-spin, spin-orbit, and tensor interactions. The momentum dependence of the amplitudes  $\Phi$  and  $\Psi$  in momentum space with width parameters  $\beta$  and  $\alpha$  are taken as

$$\Phi(k_1, k_2) = \left(\frac{1}{\pi\beta^2}\right)^{3/2} e^{-k_{rel}^2/8\beta^2}, \quad (27)$$

where  $k_{rel} = (M_{\bar{q}}k_1 - M_q k_2)/2(M_q + M_{\bar{q}})$ , and

$$\begin{aligned} \Psi_P(k_1, k_2, k_3) &= \delta^{(3)}\left(P - \sum_{i=1}^3 k_i\right) \\ &\times \left(\frac{3}{\pi\alpha^2}\right)^{3/2} e^{-\sum_{i=1}^3 (k_i - P/3)^2/2\alpha^2}. \end{aligned} \quad (28)$$

Given these, the general expression for the effective  $DN$  interaction is given as

$$V_{DN}(p, p') = \frac{1}{2} \sum_{i=1}^4 [V_i(p, p') + V_i(p', p)], \quad (29)$$

where each term in the sum corresponds to a graph in Fig. 1 given as

$$\begin{aligned} V_i(p, p') &= \left[\frac{3g}{(3+2g)\pi\alpha^2}\right]^{3/2} \int \frac{d^3q}{(2\pi)^3} v(q) e^{-a_i q^2 + b_i \cdot q} \\ &\times \left[\omega_i e^{-c_i p^2 - d_i p'^2 + e_i p \cdot p'}\right], \end{aligned} \quad (30)$$

where the  $\omega_i$  come from summing over quark color-spin-flavor quantum numbers and their values depend on spin structure of the microscopic quark interactions (see below), and the  $a_i, b_i, \dots$ , can be written as a ratio  $a_i = n(a_i)/d(a_i)\alpha^2, b_i = n(b_i)/d(b_i)\alpha^2, \dots$ . The corresponding expressions are given as follows:

Graph (1):

$$\begin{aligned} n(a_1) &= 3g, & d(a_1) &= (3+2g) \\ n(b_1) &= -g(1+4\rho)(p+p') \\ d(b_1) &= (3+2g)(1+\rho) \\ n(c_1) &= 3g^2 + 3(1+\rho)^2 + g(7+8\rho+10\rho^2) \\ d(c_1) &= 6(3+2g)(1+\rho)^2 \\ n(e_1) &= g^2 + (1+\rho)^2 - 2g(-1+\rho^2) \\ d(e_1) &= (3+2g)(1+\rho)^2, \end{aligned} \quad (31)$$

Graph (2):

$$\begin{aligned} n(a_2) &= g(3+g), & d(a_2) &= 2(3+2g) \\ n(b_2) &= g[(2+g+2\rho)p - (1+g-2\rho)p'] \\ d(b_2) &= (3+2g)(1+\rho) \\ n(c_2) &= n(c_1), & d(c_2) &= d(c_1) \\ n(d_2) &= n(d_1), & d(d_2) &= d(d_1) \\ n(e_2) &= n(e_1), & d(e_2) &= d(e_1), \end{aligned} \quad (32)$$

Graph (3):

$$\begin{aligned} n(a_3) &= 6+7g, & d(a_3) &= 4(3+2g) \\ n(b_3) &= -3[1+g+(1+2g)\rho]p \\ &\quad + [3+g+(3-2g)\rho]p' \\ d(b_3) &= 2(3+2g)(1+\rho) \\ n(c_3) &= 3g^2 + 3(1+\rho)^2 + g(7+8\rho+10\rho^2) \\ d(c_3) &= 6(3+2g)(1+\rho)^2 \\ n(d_3) &= n(c_3), & d(d_3) &= d(c_3) \\ n(e_3) &= n(e_1), & d(e_3) &= d(e_1), \end{aligned} \quad (33)$$

Graph (4):

$$\begin{aligned} n(a_4) &= 2+g, & d(a_4) &= 4 \\ n(b_4) &= -(1+g+\rho)(p-p') \\ d(b_4) &= 2(1+\rho) \\ n(c_4) &= n(c_1), & n(d_4) &= n(d_1) \\ d(c_4) &= d(c_1), & d(d_4) &= d(d_1) \\ n(e_4) &= n(e_1), & d(e_4) &= d(e_1). \end{aligned} \quad (34)$$

In these,  $g = \alpha^2/\beta^2$  and  $\rho = M_u/M_c$ .

#### IV. NUMERICAL RESULTS

Initially we solve the gap equation, Eq. (10). For the Coulomb part of the interaction,  $V$ , we employ the expression

derived in Ref. [4], which uses a quasi-particle self-consistent treatment of the gluonic vacuum – see also Ref. [13]. The numerical solution of the quasi-particle gap equation leads to an expression for  $V$  that can be parametrized in momentum space as

$$V(q) = \begin{cases} C(q) = -\frac{8.07}{q^2} \frac{\log^{-0.62}(q^2/m_g^2 + 0.82)}{\log^{0.8}(q^2/m_g^2 + 1.41)} & \text{for } q > m_g \\ L(q) = -\frac{12.25}{q^2} \left(\frac{m_g}{q}\right)^{1.93}, & \text{for } q < m_g \end{cases} \quad (35)$$

where  $m_g$  is a free parameter that comes from renormalization and sets the scale of the theory. In Ref. [4],  $m_g$  was fitted to the ground state static potential of heavy quarks. The value extracted was  $m_g = 600$  MeV. For  $U(q)$ , we the potential for the interaction of transverse gluons in momentum space, we use the following expression extracted from a fit of a lattice simulation of QCD in the Coulomb gauge [5]

$$U(q) = -\frac{q^2}{q^4 + m_G^4}, \quad (36)$$

where  $m_G$  is the Gribov mass. This is motivated by the Gribov ansatz [14] that the equal-time correlation function of transverse gluon fields  $D_{ij}^T(q)$  should vanish at  $q = 0$ . The value quoted in Ref. [5] for  $m_G$ , using the string tension as scale  $\sqrt{\sigma} = 440$  MeV to fix the lattice spacing in physical units, was  $m_G = 768$  MeV.

For discussions on the solution of the gap equation for a confining interaction like in Eq. (35), see Refs. [15, 16]. Using the value of Ref. [4] for  $m_g$ , one obtains that the solution of the gap equation gives a too small value for the quark condensate, of the order of  $\langle \bar{q}q \rangle = (-100 \text{ MeV})^3$ . Now, adding the transverse-gluon interaction,  $H_T$ , with  $U$  given by the lattice form, and using  $m_g = m_G$ , one obtains a quark condensate close to the physical value. The improvement in the value of quark condensate with the addition of a transverse part has also been found in Ref. [11]. Our results for the constituent quark mass function  $M_k$  – normalized to  $M = M_{k=0}$  – for different values of the current quark mass  $m_0$  is shown in Fig. 2 as a function of the momentum scaled to  $m_g$ . The same interaction was used to study the baryon density dependence of the quark condensate [16], with the result that the chiral restoration comes out at a too low density.

In this paper we concentrate on the elastic process  $p + \bar{D}^0 \rightarrow p + \bar{D}^0$  – the other quark-interchange processes will be discussed in a separate publication. In terms of color-spin-flavor matrix elements, this quark-interchange process is equivalent to the elastic process  $K^+ p$ , discussed in Ref. [17]. The most important contributions of  $H_4$  to this channel come from the momentum dependent central and spin-spin (proportional to  $S_1 \cdot S_2$ ) components, for which

$$v_c(q) = V(q), \quad v_\sigma(q) = \frac{2q^2}{3MM'} U(q), \quad (37)$$

where  $M' = M_u = M_d$  for graphs (1) and (3), and  $M' = M_c$  for graphs (2) and (4). The corresponding color-spin-flavor coefficients  $\omega_i$  for these interactions are shown in Table I.

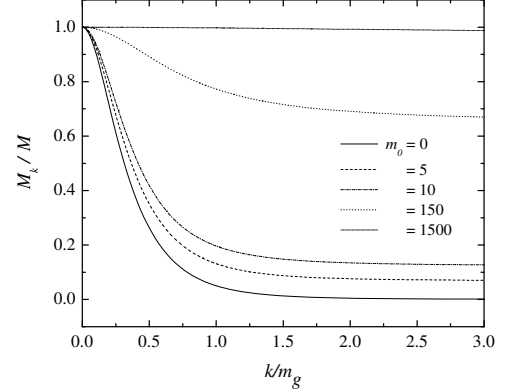


FIG. 2: The constituent quark mass function  $M_k$ , normalized to  $M = M_{k=0}$  as a function of the momentum (scaled to  $m_g$ ), for different values of the current quark mass  $m_0$ .

| qq interaction | $\omega_1$ | $\omega_2$ | $\omega_3$ | $\omega_4$ |
|----------------|------------|------------|------------|------------|
| Central        | - 4/9      | 4/9        | 4/9        | -4/9       |
| Spin-spin      | - 1/3      | -1/3       | -1/18      | -1/18      |

TABLE I: The color-spin-flavor coefficients  $\omega_i$  from the central and spin-spin interactions.

We compare results with the traditional one-gluon exchange (OGE) interaction, for which the spin-spin component is given by

$$v_\sigma^{OGE}(q) = -\frac{8\pi\alpha_s}{3MM'}, \quad (38)$$

where  $\alpha_s$  is the strong coupling constant.

The expression of the total cross section is given by

$$\sigma(s) = \int_{t_{min}}^{t_{max}} dt \frac{d\sigma(s)}{dt}, \quad (39)$$

with

$$\frac{d\sigma(s)}{dt} = \frac{4\pi^5 \left[ s^2 - (M_p^2 - M_D^2)^2 \right]}{s^2 \left[ s^2 - (M_p^2 + M_D^2)^2 \right] \left[ s^2 - (M_p^2 - M_D^2)^2 \right]} |V_{DN}|^2, \quad (40)$$

where the Mandelstam  $s$  and  $t$  can be easily related to the momenta  $p$  and  $p'$  in the c.m. system.

Our results are shown in Fig. 3. In this figure we show the prediction using the Coulomb-gauge quark model, together with the corresponding result using the interaction of Eq. (38). We use standard quark model parameters for  $\alpha = 400$  MeV and  $\beta = 383$  MeV. For the charm quark mass we use  $M_c = 1600$  MeV, and for the  $u$  and  $d$  quark masses we use  $M_u =$

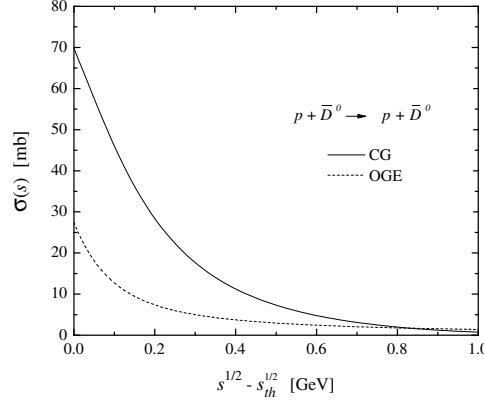


FIG. 3: Total cross-section for the elastic process  $p + \bar{D}^0 \rightarrow p + \bar{D}^0$  as a function of  $s^{1/2} - s_{th}^{1/2}$ , where  $s$  is the total c.m. energy and  $s_{th}^{1/2}$  is the threshold value of  $s$ . Solid line is for the Coulomb-gauge quark model and dashed line is for the one-gluon-exchange hyperfine interaction.

$M_d = 330$  MeV when using the OGE interaction, and  $M_u = M_d = 250$  MeV when using the Coulomb-gauge quark model.

One sees that the Coulomb-gauge quark model predicts larger values for the cross sections than the hyperfine OGE interaction. One reason for this is that the hyperfine interactions for two of the graphs in Fig. 1, come with the mass of the charm quark in the denominator, which reduces a lot the interaction at low energies. Including the Coulomb part of the OGE interaction, increases the cross section and becomes comparable to the Coulomb-gauge quark model.

## V. CONCLUSIONS AND PERSPECTIVES

In this paper we have introduced a method to calculate meson-baryon interactions in the context of a microscopic quark model inspired on the Hamiltonian of QCD in the Coulomb gauge. We used the elastic process  $p + \bar{D}^0 \rightarrow p + \bar{D}^0$  to illustrate the procedure, obtaining corresponding numerical values for the total cross section. The model contains a longitudinal Coulomb confining interaction derived from a self-consistent quasi-particle approximation to the QCD vacuum [4], and a transverse hyperfine interaction motivated from lattice simulations of QCD in Coulomb gauge [5]. The model is confining and realizes the spontaneous breaking of chiral symmetry. We have also compared results using the hyperfine component of the traditional OGE interaction, commonly used in the context of nonrelativistic quark models. We predict values above 10 mb for total cross sections close to threshold. The Coulomb-gauge quark model predicts larger values for the cross sections than the hyperfine OGE interaction, since the hyperfine interactions are suppressed by the large charm quark mass in the denominator for two quark-interchange graphs.

Our model can be improved in several respects. One direction is to use a variational estimate for the parameters  $\alpha$  and  $\beta$  optimizing the masses of the mesons and baryons. Another improvement is to avoid the expansion of the constituent quark mass function in powers of momentum, at the cost of increasing substantially the computational complexity.

## Acknowledgement

G.K. acknowledges discussions with Attilio Cucchieri, Johann Haidenbauer, Sasha Sibirtsev, and Adam Szczepaniak. Work partially supported by CNPq and FAPESP (Brazilian agencies).

- 
- [1] T. Matsui and H. Satz, Phys. Lett. B **178**, 416 (1986).
  - [2] T. Barnes, *Charmonium cross sections and the QGP*, nucl-th/0306031.
  - [3] S. Matinyan and B. Müller, Phys. Rev. C **58**, 2994 (1998); Z. Li, C.M. Ko, and B. Zhang, Phys. Rev. C **61**, 024904 (2000).
  - [4] A.P. Szczepaniak and E.S. Swanson, Phys. Rev. D **65**, 025012 (2002).
  - [5] A. Cucchieri and D. Zwanziger, Phys. Rev. D **65**, 014001 (2001).
  - [6] M.D. Girardeau, Phys. Rev. Lett. **27**, 1416 (1971); J. Math. Phys. **16**, 1901 (1975).
  - [7] D. Hadjimichef, G. Krein, S. Szpigel, and J.S. Veiga, Phys. Lett. B **367**, 317 (1996).
  - [8] D. Hadjimichef, G. Krein, S. Szpigel, and J.S. Veiga, Ann. Phys. (NY) **268**, 105 (1998).
  - [9] M.D. Girardeau, G. Krein, and D. Hadjimichef, Mod. Phys. Lett. A **11**, 1121 (1996).
  - [10] T. Barnes and E.S. Swanson, Phys. Rev. D **46**, 131 (1992); Phys. Rev. D **49**, 1166 (1994).
  - [11] F.J. Llanes-Estrada, S.R. Cotanch, A.P. Szczepaniak, and E.S. Swanson, Phys. Rev. C **70**, 035202 (2004).
  - [12] P.J.A. Bicudo, G. Krein, and J.E.F.T. Ribeiro, Phys. Rev. C **64**, 25202 (2001).
  - [13] H. Reinhardt and C. Feuchter, Phys. Rev. D **71**, 105002 (2005); W. Schleifenbaum, M. Leder, and H. Reinhardt, Phys. Rev. D **73**, 125019 (2006).
  - [14] V.N. Gribov, Nucl. Phys. B **319**, 237 (1978).
  - [15] A. Kocic, Phys. Rev. D **33**, 1785 (1985); S. Szpigel, G. Krein, and R.S. Marques de Carvalho, Braz. J. Phys. **34**, 279 (2004); AIP. Conf. Proc. **739**, 584 (2005); R. Alkofer, M. Kloker, A. Krassnigg, and R.F. Wagenbrunn, Phys. Rev. Lett. **96**, 022001 (2006).
  - [16] S.M. Antunes, G. Krein, and V.E. Vizcarra, Braz. J. Phys. **35**, 877 (2005).
  - [17] D. Hadjimichef, J. Haidenbauer, and G. Krein, Phys. Rev. C **66**, 055214 (2002).